ARMA 20–1823

Effect of non-linear elasticity on stress paths in depleted reservoirs and their surroundings

Lozovyi, S.
SINTEF, Trondheim, Norway
Yan, H. and Holt, R.M.
Norwegian University of Science and Technology, Trondheim, Norway
Bakk, A.
SINTEF, Trondheim, Norway

ABSTRACT: The prediction of stress and strain changes in and around reservoir using numerical simulators is often based on assumption of linear elasticity before reaching yield point. However, it is known that rocks are generally behaving non-linearly and a deviation from purely elastic response begins already at micro-strain level. In this work, we performed multi-scenario numerical modelling of hydrocarbon reservoir depletion using a non-linear elastic model. The model has been calibrated based on the laboratory test results with both sandstone and shale. The non-linear elastic modelling is then compared to purely linear-elastic cases. We found that assumption of pure elasticity could lead to a strong underestimation of stress and strain changes in and around the reservoir. In addition, stress path (direction of stress changes) may significantly deviate when non-linear elasticity is not accounted for.

1. INTRODUCTION

It is well-established within the petroleum industry that reservoir depletion and associated stress changes have an essential impact on field performance. Reservoir pore pressure depletion results in various stress paths in and around the reservoir. The stress path affects the geomechanical behavior, i.e. the reservoir compaction and the associated surface subsidence. Additionally, the stress changes may also cause seismic velocities alterations affecting time-lapse seismic response and providing options to monitor reservoir performance. Furthermore, the stress paths of the reservoir and the overburden are affecting the stability of boreholes during drilling and hydrocarbon production, as well as sand production.

When the stress changes in the subsurface are estimated using numerical simulators, one of the common assumptions is linear elasticity prior to the plastic yield point. Such simplification may have strong consequences on the output since it is known that rocks are not linear elastic media and a deviation from purely elastic response begins already at micro-strain level (Lozovyi et al., 2017; Winkler et al., 1979). Assumption of linear elasticity could lead to inaccurate prediction of stress-strain changes and stress path in the subsurface during e.g. hydrocarbon reservoir depletion or injection.

To this end, we performed a series of numerical simulations of a reservoir depletion in order to compare solutions computed using models for linear and non-linear elasticity. In order to calibrate the models, experimental data obtained in laboratory tests for both sandstone and shale was used. Several depletion scenarios have been tested featuring different elastic contrasts and variations of elastic and non-elastic properties for the reservoir and surroundings.

The main objective of this study is to demonstrate what consequences the assumption of linear elasticity may have on the prediction of stress changes and strains (compaction) in the reservoir and the surrounding rocks. To the knowledge of the authors, this problem has not been studied before.

2. NUMERICAL MODEL

For this study, numerical simulations are performed by using a finite element method in DIANA with an in-built non-linear rock model. An axisymmetric model was selected, which can capture the essential geometry features with a reduced computation time as compared to a full 3D model. Fig. 1 shows the half-space model geometry and boundary conditions. The red triangles indicate that there are no movements along vertical and radial boundaries. The radius of the reservoir

surroundings is chosen to be large enough to avoid numerical impacts on simulations. The bottom of the reservoir located at a depth of 2000 m with a radius of 500 m and a thickness of 150 m. The mesh size in the reservoir and surroundings defined to be 25 m. The reservoir is assumed to be totally depleted from 35 MPa to 0 MPa in 10 computation steps.

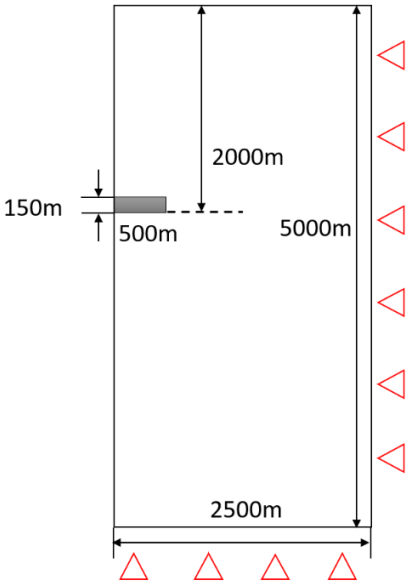

Fig. 1. The model sketch (half-space) and boundary constraints.

3. NON-LINEAR ELASTICITY

In order to model the effect of non-linear elasticity, the Jardine model (Jardine et al., 1986) has been used in this study. The model, originally developed to describe non-linear elastic behavior of soil, turned out to describe stress-strain relation for the rocks (used in this study) equally well. The model is based on a relation between the secant Young's modulus, E_u, and the axial strain, ε_a, measured in an undrained triaxial compression test. The relation is expressed in the following form:

$$E_u = G + (F - G)cos\left(\alpha\left(\log\frac{\varepsilon_a}{C}\right)^{\gamma}\right), \qquad (1)$$

where C, F, G, α, and γ are material constants that are determined by fitting the model to laboratory test data. Furthermore, parameters α, and γ are functions of additional material constants D and E: α (D, C, γ), and γ (E, D, C). This allows for direct reading of model parameters from the stiffness-strain diagram: maximum stiffness, F, at strain level C; medium stiffness, G, at strain level D; and minimum stiffness, ($2G - F$), at strain level E. Fig. 2 visualizes the fitting points and the function described by Eq. (1). When the model is fitted by experimental data, maximum and minimum stiffness points can be projected further than recorded experimental values in order to obtain the best fit.

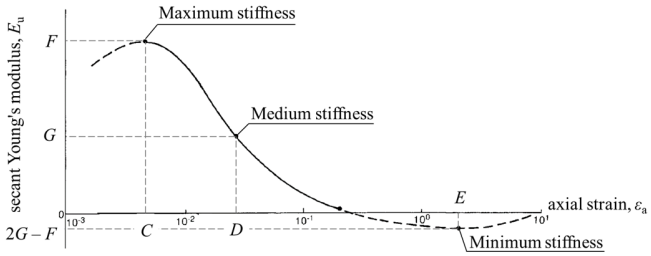

Fig. 2. Jardine parameters in stiffness-strain diagram. Modified after Jardine et al., 1986.

Several assumptions have to be done when applying the Jardine model: isotropy, constant Poisson's ratio, loading-unloading behaviour is the same (no hysteresis, observed experimentally, see e.g. Fjær et al., 2013).

The Jardine model is implemented in the finite element software DIANA used in this study to simulate reservoir depletion. In DIANA, the Jardine model is generalized by substitution of axial strain ε_a by the deviatoric strain invariant (DIANA, 2019):

$$\varepsilon_{eq} = \sqrt{\frac{2}{3^2}\left(\left(\varepsilon_1 - \varepsilon_2\right)^2 + \left(\varepsilon_2 - \varepsilon_3\right)^2 + \left(\varepsilon_3 - \varepsilon_1\right)^2\right)}, \qquad (2)$$

where ε_1, ε_2, ε_3 are principal elastic strains.

DIANA uses the following Jardine model input parameters: C, D, E, F, and G. Users also defines strain boundaries, ε_{eq_min} and ε_{eq_max}, below and above which the stiffness becomes constant and does not depend on strain (linear elastic response).

For performing numerical simulation with realistic input parameters, real experimental data has been used to calibrate the non-linear elastic model. For the reservoir, we used the experimental data obtained in confined undrained triaxial tests with Castlegate sandstone (see Lozovyi et al., 2017 for details). The Jardin non-linear elastic parameters were obtained by fitting the model to experimental data.

Fig. 3 shows both plots of Young's modulus vs. axial strain, and axial stress vs. strain. In order to study the effect of an elastic contrasts between the reservoir and surroundings, three synthetic cases for soft, medium, and stiff rock were obtained by restricting Jardine parameters of non-linearity and changing the absolute stiffness level. Table 1 shows the input parameters used in DIANA simulations. To reproduce non-elasticity for the three cases, parameters C, D, E and relation $2F - 3G = 5$ obtained for the experimental case were kept constant, as only the absolute stiffness level (parameter G in Eq. (1)) was changed.

The Jardine model has been benchmarked in DIANA in a simple triaxial loading of a cylindrical body. The response shown in Fig. 3 (red dashed curves) validates the results

of the numerical simulations. It should be noted that DIANA simulator is using drained stiffness as an input for the Jardine model.

For the surroundings of the reservoir, experimental data obtained by Lozovyi and Bauer, 2019 in confined undrained triaxial test with Opalinus Clay has been used. The work (Lozovyi and Bauer, 2019) includes experimental results for several other shales, however Opalinus Clay demonstrated the largest weakening with stress amplitude among the tested rocks. For this reason, we chose to use non-linear response of Opalinus Clay as an input data for numerical modelling to demonstrate an extreme case of non-linear elasticity in the overburden. Fig. 4 shows experimental results of triaxial loading of Opalinus Clay sample fitted with the Jardine model and modelled in DIANA thereafter.

4. RESULTS

In total, four sets of numerical simulations have been conducted: (i) the reference case using linear elastic parameters for both reservoir and surroundings, (ii) non-linear elastic surroundings and linear elastic reservoir, (iii) linear elastic surroundings and non-linear elastic reservoir, (iv) both reservoir and surroundings are non-linear elastic. Each set of simulations consisted of three variation cases which had different elastic contrast between the reservoir and surroundings. For the purpose of simplicity, the surrounding properties were unchanged and the reservoir properties had three variations (see Table 1): Stiff reservoir, medium stiff reservoir (no elastic contrast in linear-elastic case), and soft reservoir.

The results presented in this section are plotted along a vertical line that crosses the model in the center of the depleted reservoir.

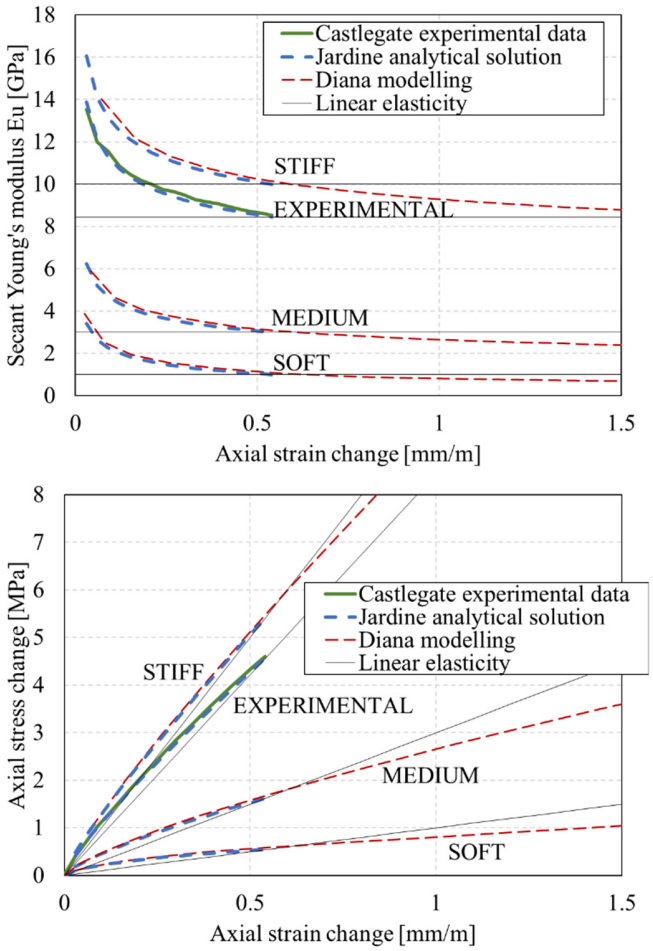

Fig. 3. Reservoir rock non-linear elastic response plots: secant Young's modulus versus axial strain (upper plot) and the corresponding axial stress versus axial strain (lower plot). The experimental data of Castlegate sandstone (green solid curve) was fitted with Jardine model analytical solution (blue dashed curve). Three synthetic stiffness-strain curves for soft, medium, and stiff rock were obtained by restricting Jardine parameters of non-linearity and changing the absolute stiffness. In this way we obtained input data for different elastic contrasts of the reservoir and surroundings and keeping the same level of non-linear elasticity. Analytical solutions were benchmarked in DIANA (red dashed curves).

Table 1. Linear and non-linear elastic material properties used for numerical simulations.

Material	Non-linear elastic parameters (Jardine model)							Linear elasticity		
	C	D	E	F	G	ε_{eq_min}	ε_{eq_max}	Young's modulus	Poisson's ratio	Density
	mm/m	mm/m	mm/m	GPa	GPa	mm/m	mm/m	GPa	-	kg/m^3
Surroundings of the reservoir	0.01	0.12	311	9.0	5.0	0.02	5	3	0.3	2300
Reservoir STIFF	0.01	0.10	182607	21.8	12.8			10		
Reservoir MEDIUM STIFF				9.3	4.5			3		
Reservoir SOFT				5.7	2.1		0.5	1		

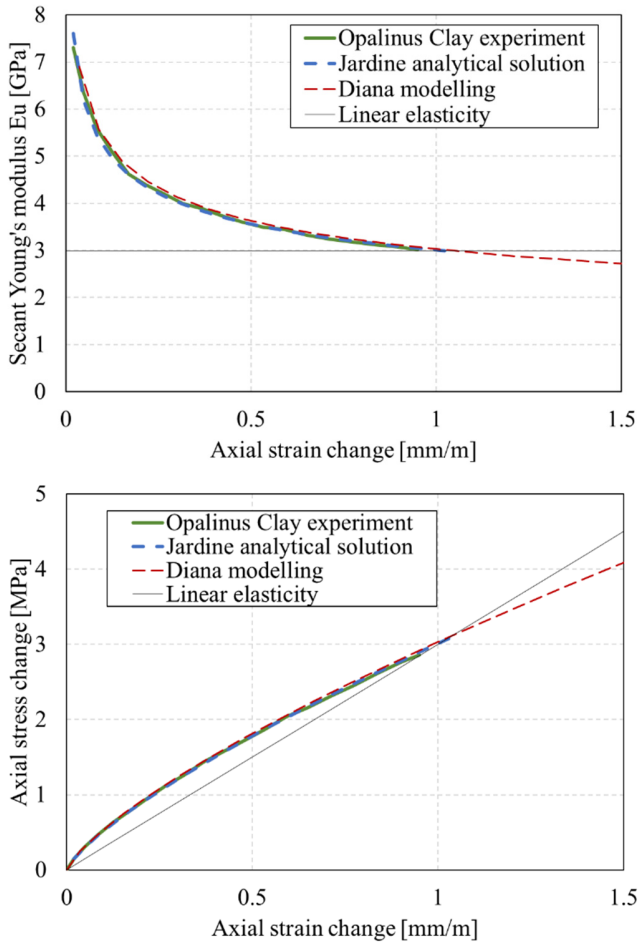

Fig. 4. Surrounding (overburden) rock non-linear elastic response plots: secant Young's modulus versus axial strain (upper plot) and the corresponding axial stress versus axial strain (lower plot). The experimental data for Opalinus Clay (green solid curve) was fitted with Jardine model analytical solution (blue dashed curve). Analytical solution was benchmarked in DIANA (red dashed curve).

4.1. Stress path coefficients

Stress path coefficients provide a way to quantitatively evaluate stress changes during reservoir depletion. For vertical and horizontal stress changes, $\Delta\sigma_v$ and $\Delta\sigma_h$ respectively, caused by pore pressure change withing reservoir ΔP_{f_res}, reservoir stress path coefficients are given by (Hettema et al., 2000):

$$\gamma_v = \frac{\Delta\sigma_v}{\Delta P_{f\_res}}, \quad \gamma_h = \frac{\Delta\sigma_h}{\Delta P_{f\_res}} \tag{3}$$

where γ_v is so-called the arching coefficient and γ_h is depletion coefficient.

Fig. 5 plots the stress path coefficients γ_v and γ_h versus depth along vertical cross section through the middle of the reservoir for three variation cases with different elastic contrasts.

Another stress path coefficient κ is introduced to characterize the direction of stress changes. Within the depleting reservoir, κ is defined as the relative changes between horizontal effective stress changes (Fjær et al., 2008):

$$\kappa_{res} = \frac{\Delta\sigma'_h}{\Delta\sigma'_v}, \tag{4}$$

here, effective stress is defined as Terzaghi's effective stress or net stress i.e. $\Delta\sigma' = \Delta\sigma - P_{f\_res}$.

For the surroundings, κ is defined as the relative change between horizontal and vertical stress changes (Holt et al., 2018), as given by:

$$\kappa_{sur} = \frac{\Delta\sigma_h}{\Delta\sigma_v}. \tag{5}$$

The κ of the reservoir surrounding for medium stiff reservoir is shown in Fig. 6. The stress path coefficient κ for the reservoir section is shown in Fig. 7.

4.2. Compaction

Pore pressure depletion leads to changes in the total stresses which control compaction and subsidence. In order to quantitatively estimate the effect of rock non-linearity on compaction, the vertical strain is plotted versus depth along a vertical cross section through the middle of the reservoir for three variation cases with different elastic contrasts (Fig. 8).

5. DISCUSSION

Before proceeding to the discussion of the results, the assumptions made in this study should be pointed out:

- Isotropy: it is known that rocks and especially shales are anisotropic which would affect the subsurface response.
- Non-linear elasticity (Young's modulus): in reality, the rock behavior is different upon loading and unloading leading to a hysteresis of the stress-strain curve, it is called non-elastic response (see e.g. Fjær et al., 2013).
- Constant Poisson's ratio: it is evident from the experiments that Poisson's ratio is also a strain (or stress) dependent parameter. For example, for Opalinus Clay, vertical Poisson's ratio increase from 0.35 to 0.46 for a 3 MPa triaxial unloading section (Lozovyi and Bauer, 2019).

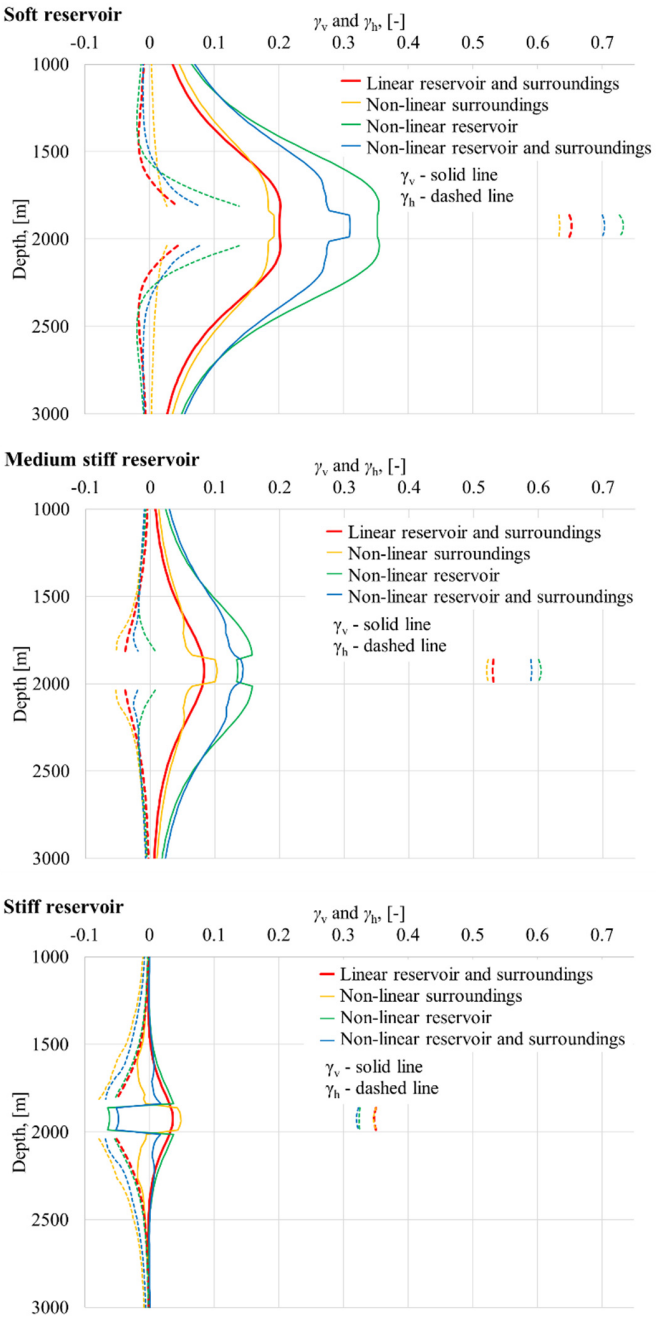

Fig. 5. Stress path coefficients γ_v (vertical) and γ_h (horizontal) plotted versus depth along vertical cross section through the middle of the reservoir for three variation cases with different elastic contrast (cf. Table 1). Solid line corresponds to γ_v, and dashed line corresponds to γ_h.

- Use of laboratory scale experimental data as input: rock samples might not be representative for the entire subsurface.

Another aspect is how the input parameters for the linear elastic model are determined. For our case, linear stiffness was obtained from the unloading part of a triaxial stress cycle with 5 MPa stress amplitudes. One may argue that if the stress changes in the field are comparable to those applied in the test, the difference between linear and non-linear cases may be negligible. However, since different

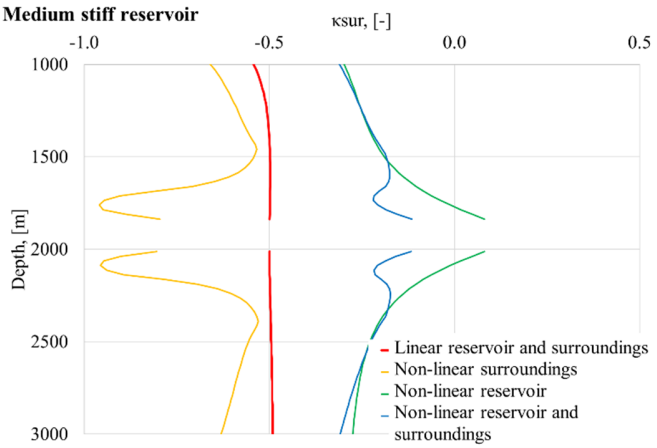

Fig. 6. Stress path coefficient κ_{sur} plotted versus depth along vertical cross section through the middle of the reservoir. For the linear elastic case there is no elastic contrast, the results are in agreement with Geertsma's analytical model solution (see discussion in section 5.2).

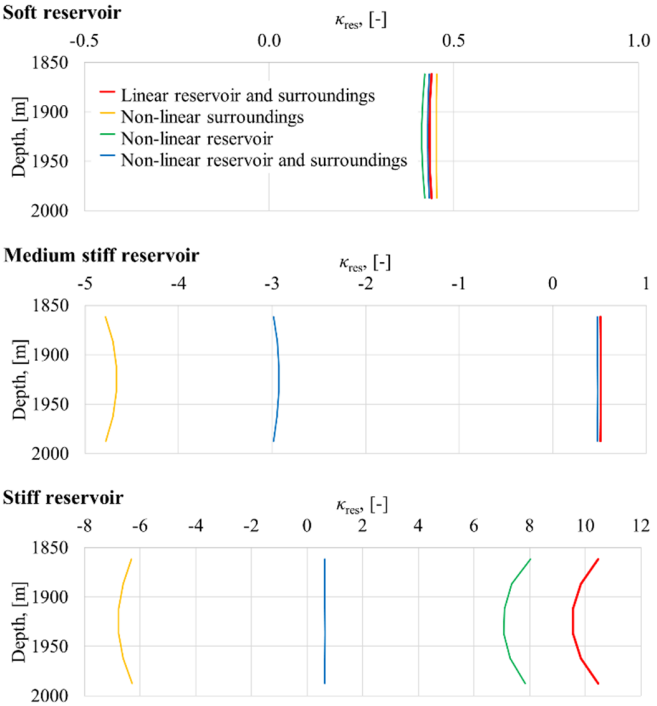

Fig. 7. Stress path coefficient κ for the reservoir section.

parts of the subsurface follow different stress paths and experience different strains leading to heterogeneous stiffness and strain changes, the overall field response would generally differ from linear (cf. Fig. 3).

Despite the simplifications, this work may be the first systematic attempt to quantify the effect of non-linear stress-strain behavior, calibrated from experimental data, in a field scale modelling.

In the following sub-sections, we describe influence of non-linearity on the prediction of stress changes, stress path, and compaction.

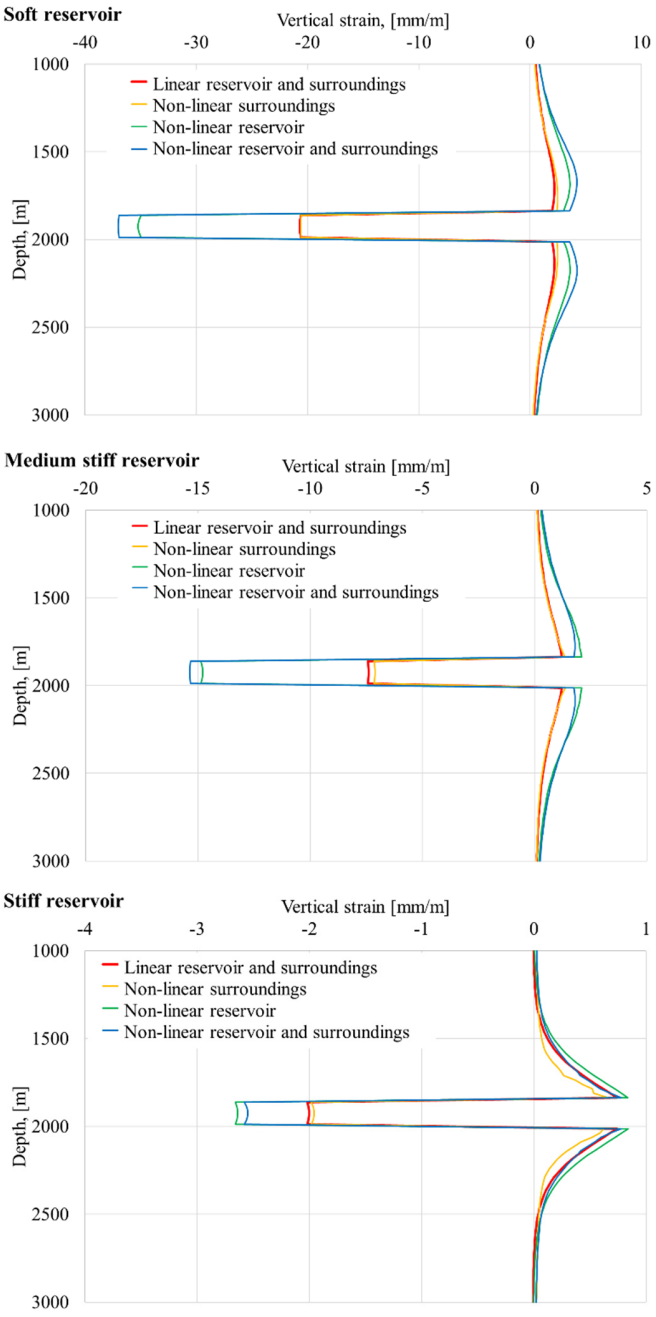

Fig. 8. Vertical strain plotted versus depth along vertical cross section through the middle of the reservoir for the three variation cases with different elastic contrast (cf. Table 1).

5.1. *Stress changes*

Analyzing the results in Fig. 5, it is evident that the non-linear behavior of the reservoir alone has a significant impact on overall subsurface response, i.e. including reservoir non-linearity in the analysis is strongly affecting not only the reservoir, but also the overburden response.

The strongest deviation in stress changes between the linear elastic and completely non-linear cases is observed for the vertical stress path coefficient both inside the reservoir and its surroundings. As for horizontal stress path, the discrepancy between non-linear and linear elastic cases is noticeable within the reservoir, but not as strong in the surroundings. The stiffness contrast steers the degree of arching, i.e. the magnitude of γ_v in the surroundings and γ_v and γ_h in the reservoir. The vertical stress path discrepancy between completely linear and non-linear models are following: for the soft reservoir case, γ_v is underestimated (here and further we refer to the linear case) by about 0.11 inside the reservoir and 0.07 for the proximal reservoir surroundings (100 m away); for the medium reservoir case, the underestimation of γ_v is about 0.06 and 0.08 for both reservoir and proximal surroundings; however, for the stiffer reservoir case, linear model considerably overestimates vertical stress path coefficient within the reservoir (by 0.09) and up to about 200 m away in the surroundings (by 0.02).

Such strong non-linear effects may cause inaccurate stress change predictions within and near the reservoir leading to a risk of fault reactivation, seismicity, as well as stability of existing wells and future drilling operations during the lifetime of the reservoir.

5.2. *Stress path*

Modeling results indicate that non-linear elasticity can strongly influence the stress path (direction of stress changes, see Eq. 4 and 5). Fig. 6 shows the stress path coefficient κ for the surrounding rock. For the linear elastic case, the numerical solution (red line on Fig. 6) is in agreement with the analytical solution of Geertsma, 1973. Geertsma's linear-elastic model considers a horizontally oriented disk-shaped reservoir with no elastic contrast between the reservoir and its surroundings, the mean stress is approximately constant everywhere outside the reservoir and $\kappa_{sur} = -1/2$ (see also Fjær et al., 2008; Ch. 12). However, non-elasticity of the reservoir and surroundings shifts the stress path closer to a pure vertical (uniaxial) stress changes. Even more dramatic effect of non-linearity on the stress path is observed within the reservoir (Fig. 7).

In previous studies (Morita et al., 1989; Mulders, 2003) it was found that arching is promoted if the stiffness of the depleting reservoir is significantly lower than of the surrounding rock. In our study we found that the assumption of linear elasticity (compared to non-linear elasticity) could lead to underestimation of the arching effect. We observe that in the non-linear elastic cases, the reservoir could increase arching due to gradual sandstone softening. This effect in turn alters the stress path.

5.3. Reservoir compaction

Our modelling results show that for all variation cases, axial strain is underestimated by a linear-elastic model inside the reservoir. The results are shown in Fig. 8 are summarized in Table 2 for strains in the center of a disc-shaped reservoir. For the soft reservoir case, linear-elastic model has underpredicted vertical strain by 15 mStrain compared to non-linear elastic model. For the medium stiff reservoir case, this difference is 8 mStrain. The stiff reservoir case does not show too strong difference between linear and non-linear model predictions.

Table 2. Vertical strain in the center of the depleted reservoir compared for the linear-elastic and non-linear elastic model scenarios.

	Vertical strain [mm/m]		
	Soft reservoir	Medium stiff reservoir	Stiff reservoir
Linear reservoir and surroundings	-21.6	-7.4	-2.0
Non-linear reservoir and surroundings	-37.0	-15.4	-2.5

Since the pore pressure is reduced during depletion only within the reservoir, a reservoir drained response is responsible for most of the non-linear driven deformation. The consequence of underestimating the compaction may significantly bias the interpretation of time-lapse seismic surveys, causing well instabilities, fault reactivation, errors are in fluid flow performance predictions, reservoir permeability and the directions of preferred flow.

6. CONCLUSIONS

The aim of this work was to investigate the impact of non-linear elasticity (that is often observed empirically for rocks) on stress and strain change predictions in and around a depleting reservoir. We have performed a series of numerical simulations of a synthetic field depletion case using finite element simulation, where a non-linear elastic model calibrated from laboratory data was utilized. The non-linear elastic modelling was then compared to purely linear-elastic cases. We found that the assumption of pure elasticity could lead to strong underestimation of stress and strain changes in and around the reservoir, both qualitatively and quantitatively as manifested in the horizontal and vertical stress path coefficients. It is found that non-linear behavior of the reservoir is dominating in overall subsurface response, i.e. affecting both overburden and reservoir. In addition, the stress path (ratio between the horizontal and vertical stress changes) may significantly deviate when the non-linear elasticity is not accounted for. A natural continuation of this work would be implementation of more advanced constitutive non-linear models and to study this in context with elastic anisotropy.

ACKNOWLEDGEMENT

We thank the Research Council of Norway through the PETROMAKS2 programme (Grant 294369), AkerBP, Equinor, and Shell for funding in the project: Improved prediction of stress and pore-pressure changes in the overburden for infill drilling.

REFERENCES

1. Fjær, E., Holt, R.M., Horsrud, P., Raaen, A.M., and Risnes, R. 2008. *Petroleum Related Rock Mechanics*. 2nd ed.: Elsevier.

2. Fjær, E., Stroisz, A.M., and Holt, R.M. 2013. Elastic Dispersion Derived from a Combination of Static and Dynamic Measurements. Rock Mechanics and Rock Engineering 46, 611–618.

3. Geertsma, J. 1973. A basic theory of subsidence due to reservoir compaction: The homogeneous case. *Verhandelingen Kon. Ned. Geol. Mijnbouwk* 28, 43–62.

4. Hettema, M.H.H., Schutjens, P.M.T.M., Verboom, B.J.M., and Gussinklo, H.J. 2000. Production-Induced Compaction of a Sandstone Reservoir: The Strong Influence of Stress Path. *SPE Reservoir Evaluation & Engineering* 3, 342–347.

5. Holt, R.M., Bauer, A., and Bakk, A. 2018. Stress-path-dependent velocities in shales: Impact on 4D seismic interpretation. *GEOPHYSICS* 83, MR353–MR367.

6. Jardine, R.J., Potts, D.M., Fourie, A.B., and Burland, J.B. 1986. Studies of the influence of non-linear stress–strain characteristics in soil–structure interaction. *Géotechnique* 36, 377–396.

7. Lozovyi, S., and Bauer, A. 2019. From Static to Dynamic Stiffness of Shales: Frequency and Stress Dependence. *Rock Mech Rock Eng.* 52: 5085–5098.

8. Lozovyi, S., Sirevaag, T., Szewczyk, D., Bauer, A., and Fjær, E. 2017. Non-elastic effects in static and dynamic rock stiffness. In *Proceedings of the 51st US Rock Mechanics/Geomechanics Symposium, San Francisco, USA*.

9. Morita, N., Whitfill, D.L., Nygaard, O., and Bale, A. 1989. A Quick Method To Determine Subsidence, Reservoir Compaction, and In-Situ Stress Induced by Reservoir Depletion. *Journal of Petroleum Technology* 41, 71–79.

10. Mulders, F.M.M. 2003. Modelling of stress development and fault slip in and around a producing gas reservoir. DUP Science.

11. Winkler, K., Nur, A., and Gladwin, M. 1979. Friction and seismic attenuation in rocks. *Nature* 277: 528–531.

12. DIANA. 2019. DIANA – Finite Element Analysis Release Notes release 10.3. ed. Denise Ferreira, 18.2.3. DIANA FEA bv.